

# Antiferromagnetic topological insulator state in the correlated Bernevig-Hughes-Zhang model

S. Miyakoshi and Y. Ohta

*Department of Physics, Chiba University, Chiba 263-8522, Japan*

(Dated: 15 March 2013)

We study the effects of electron correlations on the topological phase transition in the Bernevig-Hughes-Zhang model using the variational cluster approach where the short-range spatial correlations are taken into account exactly. We calculate the spin Chern number and local magnetic moment to show that the topologically nontrivial antiferromagnetic order exists and that the magnetic transition is of the second order. We furthermore demonstrate that under the spin-quantized condition the topological phase transition is caused by the closing of the bulk band gap.

PACS numbers: 73.43.Nq, 71.10.Fd, 71.30.+h

## I. INTRODUCTION

Presence of the topologically ordered phases<sup>1,2</sup> has received much attention in recent years from both theoretical and experimental sides. The existence of gapless edge states and their characteristic electromagnetic responses detected in, e.g., the quantum Hall systems<sup>3,4</sup> have been understood in terms of the topological orders and their unconventional insulator states distinguished from the simple insulator states by their nontrivial topological structure have been broadly referred to as the topological insulators (TIs).<sup>5,6</sup> Experimentally, the  $\mathbb{Z}_2$  topological band insulators (TBIs),<sup>7–16</sup> which are caused by the spin-orbit coupling without external magnetic field, have been realized in two- and three-dimensional systems such as HgTe/CdTe quantum wells<sup>10,13</sup> and bismuth based compounds.<sup>14–16</sup> Their gapless edge states are protected by the time-reversal symmetry and their topology is reflected in the parity of the number of the edge states.<sup>17–19</sup> The relation between the crystallographic symmetry of the system and the presence of topologically ordered states in such systems has thus been studied intensively in recent years.<sup>20–22</sup>

The studies of the TBIs have been made within the noninteracting band theory on one hand. However, the introduction of electron correlations to the TBIs has on the other hand attracted great attention from the viewpoint of the possible realization of exotic topological phases.<sup>23–34</sup> In recent studies, a number of candidates for the exotic topologically ordered phases, where both the spin-orbit interaction and electron correlations play essential roles, have been proposed in transition-metal oxides, such as iridium oxides.<sup>23,24</sup> For such systems, the properties of the TBIs, which reflect the effects of electron correlations and competition between the antiferromagnetic (AF) and topological orders, have been clarified in a wide variety of numerical methods, such as variational Monte Carlo (VMC) method,<sup>26</sup> quantum Monte Carlo (QMC) method,<sup>27</sup> dynamical mean-field theory (DMFT),<sup>28–31</sup> variational cluster approach (VCA),<sup>32</sup> and cluster dynamical mean-field theory (CDMFT).<sup>33</sup> In particular, in the DMFT study<sup>29</sup> of the Bernevig-Hughes-

Zhang (BHZ) model<sup>10</sup> reproducing the TBI state, the coexistence of the TBI and axial antiferromagnetic Mott insulator (AFMI) state has been confirmed by including the on-site Hubbard interaction, the state of which is called the antiferromagnetic topological insulator (AFTI). In the QMC study<sup>27</sup> of the Kane-Mele model,<sup>8,9</sup> another model reproducing the TBI state, it was found that the topological phase transition between the TBI and in-plane AFMI also appears but occurs without closing of the bulk band gap. The difference in the topological phase transitions between these two models has been understood as a consequence of the symmetry that conserves the  $z$ -component of the total-spin quantum numbers of the system, i.e., the spin-quantized condition.<sup>34</sup>

However, because the spatial electron correlations cannot be treated sufficiently in the DMFT framework, the study of their effects on the AFTI states in the BHZ model still remains to be an important issue. In this paper, we will therefore apply the method of VCA<sup>35–39</sup> to the BHZ model extended with the on-site Hubbard interaction, whereby we can treat the short-range spatial correlations exactly and calculate the single-particle Green function directly. We will thus evaluate the spin Chern number (SChN)<sup>28–30,40,41</sup> and local magnetic moment of the AF order and show that the AF state actually has the topologically nontrivial structure, i.e., the AFTI state exists, under the spin-quantized condition. We will furthermore show that the magnetic transition between the TBI and AFTI is of the second order and will demonstrate that the topological phase transition between the AFTI and AFMI occurs with closing of the bulk band gap.

This paper is organized as follows: In Sec. II, we introduce the extended BHZ model with the on-site Hubbard interaction and briefly discuss the method of calculation. In Sec. III, we first calculate the properties of SChN and single-particle spectrum for the bulk and edge states in the nonmagnetic case and confirm that the result for SChN can determine the topological phase transition point in agreement with the single-particle spectra. We then show the results for the AF ordered case and discuss the property of the topologically nontrivial AF order, including the influences on the single-particle

spectra and local magnetic moments. A summary of the paper is given in Sec. IV.

## II. MODEL AND METHOD

We study the BHZ model<sup>10</sup> defined on the two-dimensional square lattice with an extension of includ-

ing the on-site Hubbard interaction  $U$ . The Hamiltonian reads

$$\mathcal{H} = \mathcal{H}_{\text{BHZ}} + \mathcal{H}_{\text{int}} = \sum_{ij} \hat{c}_i^\dagger \hat{\mathcal{H}}_{ij} \hat{c}_j + U \sum_{i\alpha} n_{i\alpha\uparrow} n_{i\alpha\downarrow} \quad (1a)$$

$$\hat{\mathcal{H}}_{ij} = \begin{pmatrix} \mathcal{H}_{ij} & 0 \\ 0 & \mathcal{H}_{ij}^* \end{pmatrix} \quad (1b)$$

$$\mathcal{H}_{ij} = \begin{pmatrix} \epsilon_1 \delta_{i,j} + t_1 (\delta_{i,j+\hat{x}} + \delta_{i,j+\hat{y}}) & t' [i(\delta_{i,j+\hat{x}} - \delta_{i,j-\hat{x}}) + \delta_{i,j+\hat{y}} - \delta_{i,j-\hat{y}}] \\ t' [i(\delta_{i,j+\hat{x}} - \delta_{i,j-\hat{x}}) + \delta_{i,j-\hat{y}} - \delta_{i,j+\hat{y}}] & \epsilon_2 \delta_{i,j} + t_2 (\delta_{i,j+\hat{x}} + \delta_{i,j+\hat{y}}) \end{pmatrix} \quad (1c)$$

where  $\hat{c}_i = (c_{i1\uparrow}, c_{i2\uparrow}, c_{i1\downarrow}, c_{i2\downarrow})^T$  and  $n_{i\alpha\sigma} = c_{i\alpha\sigma}^\dagger c_{i\alpha\sigma}$ . This Hamiltonian contains two orbitals  $\alpha = 1, 2$  and spin  $\sigma = \uparrow, \downarrow$ . The off-diagonal term in  $\mathcal{H}_{ij}$ , which corresponds to the spin-orbit coupling, is illustrated in Fig. 1. In our calculation, we consider the particle-hole symmetric case, assuming  $-t_1 = t_2 = t$ ,  $-\epsilon_1 = \epsilon_2 = t$ , and  $t' = 0.8t$ .

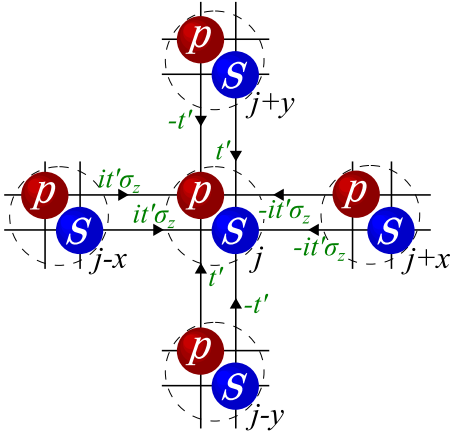


FIG. 1: (Color online) Schematic illustration of the spin-orbit coupling term in the BHZ model. The circles labeled “s” and “p” correspond to the orbital  $\alpha = 1$  (s) and orbital  $\alpha = 2$  (p), respectively.  $j$ ,  $j \pm x$ , and  $j \pm y$  denote the lattice sites.

The VCA is a quantum cluster method based on the self-energy functional theory (SFT)<sup>35,36</sup> and has been applied to many interesting problems that include the competition between the symmetry-broken phases such as the superconducting phase, antiferromagnetic phase, etc. In the SFT framework, the problem of calculating the exact self-energy becomes a variational problem for the grand

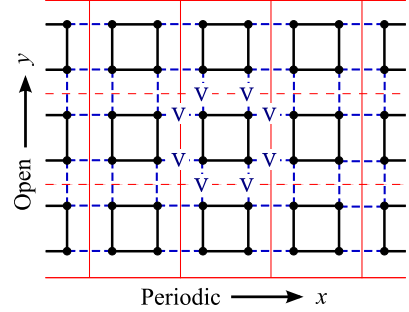


FIG. 2: (Color online) Sketch of the tiling used for calculating the single-particle spectrum for the edge. The dotted line represents the inter-cluster hopping term  $\mathbf{V}$ . We use the 4-site cluster for the bulk and edge states in the VCA calculations. To see the edge states, we arrange 10 clusters along the  $y$  axis.

potential functional  $\Omega[\Sigma]$  defined as

$$\Omega[\Sigma] = \text{Tr} \ln(\mathbf{G}_0^{-1} - \Sigma)^{-1} + F[\Sigma] \quad (2)$$

where  $F[\Sigma]$  is the Legendre transform of the Luttinger-Ward functional  $\Phi[\mathbf{G}]$  such that the condition  $\delta F[\Sigma] = -T\mathbf{G} \cdot \delta\Sigma$  is satisfied, and therefore, the condition  $\delta\Omega[\Sigma] = 0$  corresponds to the Dyson equation  $\mathbf{G}^{-1} = \mathbf{G}_0^{-1} - \Sigma$ .  $\text{Tr}$  in Eq. 2 represents both the sum over the Matsubara frequency and trace over the single-particle bases, such as momentum, spin, orbital, etc. In particular, the self-energy  $\Sigma$  can be obtained in VCA, where we use the reference system consisting of the small clusters with the single-particle parameters  $\mathbf{t}'$ , which are chosen so as to satisfy the stationary condition of the grand potential functional  $\Omega[\Sigma'(\mathbf{t}')]$ . Furthermore, if we introduce the Weiss field as a variational parameter, we can treat the spontaneous symmetry breaking. In the VCA framework, the grand potential functional  $\Omega[\Sigma'(\mathbf{t}')]$  can

be rewritten as

$$\Omega[\Sigma'(\mathbf{t}')] = \Omega'(\mathbf{t}') - \text{Tr} \ln[\mathbf{G}'(\mathbf{t}')] + \text{Tr} \ln[\mathbf{G}_0^{-1} - \Sigma'(\mathbf{t}')]^{-1} \quad (3)$$

where  $\Omega'(\mathbf{t}') - \text{Tr} \ln[\mathbf{G}'(\mathbf{t}')] corresponds to  $F[\Sigma'(\mathbf{t}')] in the reference system, and  $\mathbf{G}_0$  is the free propagator of the original lattice system. Details of VCA can be found in Refs. 38 and 39.$$

In the evaluation of the SChN and single-particle spectrum, we use the cluster perturbation theory (CPT)<sup>37</sup> to calculate the lattice Green function  $\mathbf{G}(\mathbf{t}')$ , which is given by

$$\begin{aligned} \mathbf{G}(\mathbf{t}') &= [\mathbf{G}_0^{-1} - \Sigma'(\mathbf{t}')]^{-1} \\ &= [\mathbf{G}_0^{-1} - \mathbf{G}_0^{-1}(\mathbf{t}') + \mathbf{G}_0^{-1}(\mathbf{t}') - \Sigma'(\mathbf{t}')]^{-1} \\ &= [-\mathbf{V} + \mathbf{G}'^{-1}(\mathbf{t}')]^{-1} \\ &= \mathbf{G}'(\mathbf{t}')[\hat{1} - \mathbf{V}\mathbf{G}'(\mathbf{t}')]^{-1} \end{aligned} \quad (4)$$

where  $\mathbf{V}$  is the inter-cluster hopping treated perturbatively. In the calculation of the bulk states, we use the supercluster where the clusters are arranged along the  $x$  and  $y$  axes and connected periodically along both directions. For the edge states, on the other hand, we use the supercluster where the clusters are arranged along the  $x$  and  $y$  axes but connected periodically only along the  $x$  axis (see Fig. 2).

The SChN, which characterizes the topological property in the bulk states, may be written in the Green function formalism<sup>25,28,29,40</sup> as

$$N = \frac{\epsilon_{\mu\nu\rho}}{48\pi^2} \int d^3k \text{Tr}[\hat{\sigma}_z \mathbf{G}(k) \partial_\mu \mathbf{G}^{-1}(k) \times \mathbf{G}(k) \partial_\nu \mathbf{G}^{-1}(k) \mathbf{G}(k) \partial_\rho \mathbf{G}^{-1}(k)] \quad (5)$$

where the notation  $k = (i\omega, \mathbf{k})$  is used,  $\partial_\mu$  denotes the partial differentiation with respect to  $k^\mu$ , and  $\epsilon_{\mu\nu\rho}$  is the antisymmetric symbol. This quantity is in proportion to the spin Hall conductivity and has the quantized value as long as the total spin  $S_{\text{tot}}^z$  of the system is conserved.<sup>42,43</sup> In general, the  $\mathbb{Z}_2$  topological insulator is characterized by  $\mathbb{Z}_2$  invariant, which is well-defined as long as the time-reversal symmetry remains. The SChN on the other hand is equivalent to the parity of  $\mathbb{Z}_2$  invariant on the condition of the spin conservation and is applicable to the axial AF case where the time-reversal symmetry is broken.

Here, let us consider the SChN in the noninteracting BHZ model for simplicity. In this case, SChN can be divided into the up- and down-spin parts as  $N = N_\uparrow - N_\downarrow$ , and the spin-polarized Hamiltonian  $\hat{\mathcal{H}}_\sigma$  can be written in  $\mathbf{k}$  space in the matrix form as

$$\hat{\mathcal{H}}_\sigma(\mathbf{k}) = \sum_i d_i(\mathbf{k}) \hat{\tau}_i \quad (6a)$$

$$d_1(\mathbf{k}) = -2t' \sin k_x \times \text{sign}(\sigma) \quad (6b)$$

$$d_2(\mathbf{k}) = -2t' \sin k_y \quad (6c)$$

$$d_3(\mathbf{k}) = -t - 2t(\cos k_x + \cos k_y) \quad (6d)$$

where  $\hat{\tau}_i$  represents the Pauli matrix for the orbital degrees of freedom. Eq. (5) can then be rewritten in terms of the  $\sigma$ -spin contributions to the spin Chern number

$$N_\sigma = -\frac{1}{8\pi} \int d^2\mathbf{k} \hat{d}(\mathbf{k}) \cdot \partial_{k_x} \hat{d}(\mathbf{k}) \times \partial_{k_y} \hat{d}(\mathbf{k}) \quad (7)$$

with  $\hat{d}_i = d_i/|\hat{d}|$ . Using Eq. (7), we obtain SChN as  $N = 1$  with  $N_\uparrow = -N_\downarrow = 1/2$ , where the sign of SChN is determined from the sign of the spin-orbit interaction terms of Eqs. (6b) and (6c) and reflects the direction of the current carried by the helical edge states.

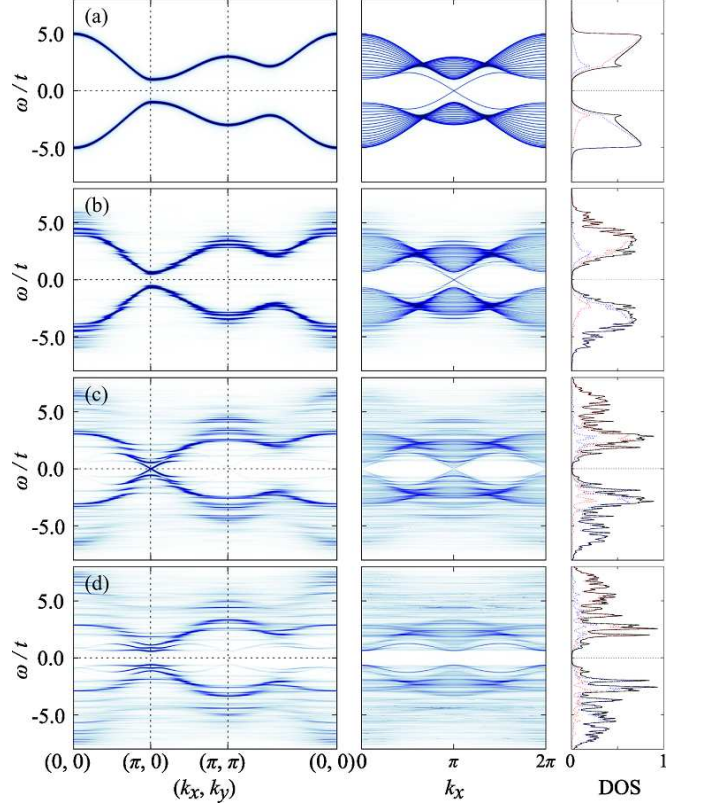


FIG. 3: (Color online) Single-particle spectra for the bulk (left panel) and edge state (middle panel) calculated by CPT. Right panel shows the density of states (DOS) for the bulk. The characteristic values of  $U$  used are: (a)  $U = 0$  (TBI), (b)  $U = 2.0t$  (TBI), (c)  $U = 4.4t$  (topological phase transition point), and (d)  $U = 6.0t$  (NMI).

### III. RESULTS OF CALCULATION

First, we discuss the effects of the on-site Hubbard interaction  $U$  on the BHZ model in the nonmagnetic case. Figure 3 shows the results for the single-particle spectra of the bulk and edge states. At  $U < 4.4t$ , we find that the band gap in the bulk state (which we call the bulk gap) and the gapless edge state appear, which characterize the topologically nontrivial state, and thus we confirm that this region  $U < 4.4t$  belongs to the TBI

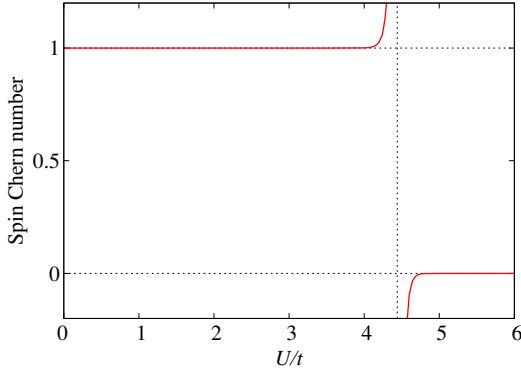


FIG. 4: (Color online) Calculated SChN for the nonmagnetic state. The vertical dotted line at  $U = 4.4t$  indicates the topological phase transition point between the TBI and NMI states.

state. Then, at  $U = 4.4t$ , the bulk gap closes and simultaneously the gapless edge state vanishes (bulk-edge correspondence), indicating that the electron correlation  $U$  derives the topological phase transition. At  $U > 4.4t$ , the bulk gap opens again but no gapless edge state appears, and thus the system belongs to the trivial nonmagnetic insulator (NMI) state. Interestingly, this phase transition occurs with closing the bulk gap and the single-particle spectrum for the bulk state acquires the linear dispersion. This result has also been observed in the VCA study of the Kane-Mele model. Therefore, in general, the closing of the bulk gap becomes a signal of the appearance of the topological phase transition between the TBI and NMI states.

We note here that, although the single-particle spectra for the bulk and edge states are useful for detecting the topological phase transition as shown above, we cannot verify in this calculation whether the edge state actually brings the quantized spin current. Also, it is not easy to take into account the possible inhomogeneity of the self-energies in the edge states in the VCA calculation. The SChN is free from such problems when we characterize the topology of the bulk states in correlated systems, which we will show in the following.

The calculated result for SChN is shown in Fig. 4, where we find that, with increasing  $U$ , SChN discontinuously changes from 1 to 0 with a divergence at  $U = 4.4t$ . This behavior corresponds to the bulk-gap closing at  $U = 4.4t$  shown in Fig. 3. In general, without any bulk-gap closing or anomaly of the self energy, the topological properties of the system do not change.<sup>25,29</sup> Therefore, this result also indicates that the topological phase transition between the TBI and NMI states occurs simultaneously with the bulk-gap closing. In other words, this result supports the validity of our calculation of the single-particle spectra for the edge state. Note that our result for SChN does not show a step-function-like behavior from 1 to 0 but rather show a diverging behavior deviating from 1 or 0 in the vicinity of the transition

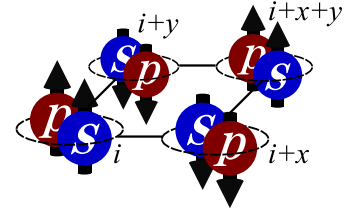


FIG. 5: (Color online) Schematic representation of the magnetic ordering in the BHZ model. The spheres labeled “s” and “p” correspond to the orbital  $\alpha = 1$  (or s) and orbital  $\alpha = 2$  (or p), respectively, and the arrows indicate the spin directions.

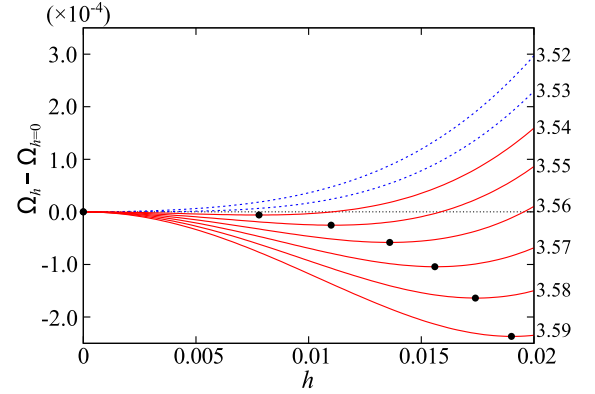


FIG. 6: (Color online) Calculated grand potential  $\Omega_h - \Omega_{h=0}$  (per site) as a function of the Weiss field  $h$  at several values of  $U$ . The value of  $U$  used is shown on each curve. The dots indicate the stationary points.

point. This is due to a numerical error, which is however not serious for determining the topological phase transition point because the divergence of SChN signals the transition point accurately. This method of SChN can thus be used to determine the topological phase transition point between two topologically distinct states even when the system has the AF order, as we will discuss in the following.

Next, we discuss the magnetic instability in the BHZ model induced when we introduce the Hubbard interaction  $U$ . Let us first consider the case at large- $U$  limit, whereby we can search for candidates of the magnetic instabilities. Our model in this case may be rewritten by the following spin Hamiltonian:

$$\mathcal{H} = \sum_{\langle i,j \rangle \alpha \beta} \left[ J_{ij;\alpha\beta} \mathbf{S}_{i\alpha} \cdot \mathbf{S}_{j\beta} - 2J_{ij;\alpha\beta}^{xy} (S_{i\alpha}^x S_{j\beta}^x + S_{i\alpha}^y S_{j\beta}^y) \right] \quad (8a)$$

$$J_{ij;\alpha\beta} = \left( \frac{4t^2}{U} \delta_{\alpha\beta} + \frac{4t'^2}{U} (1 - \delta_{\alpha\beta}) \right) (\delta_{ij\pm x} + \delta_{ij\pm y}) \quad (8b)$$

$$J_{ij;\alpha\beta}^{xy} = \frac{4t'^2}{U} \delta_{ij\pm x} (1 - \delta_{\alpha\beta}) \quad (8c)$$

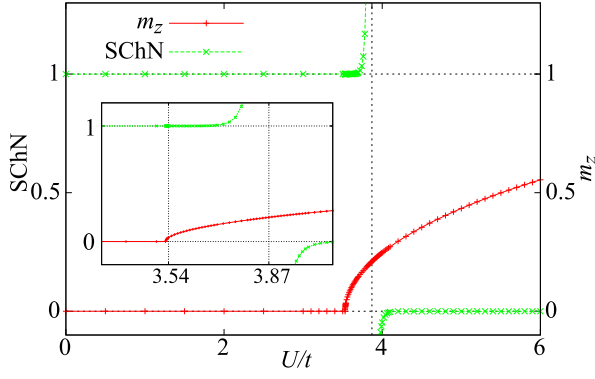


FIG. 7: (Color online) Calculated spin Chern number (SChN) and local magnetic momentum  $m_z$ . The vertical dotted line at  $U=3.87t$  indicates the topological phase transition point between the AFTI and AFMI states. The inset enlarges the region near the phase transition points.

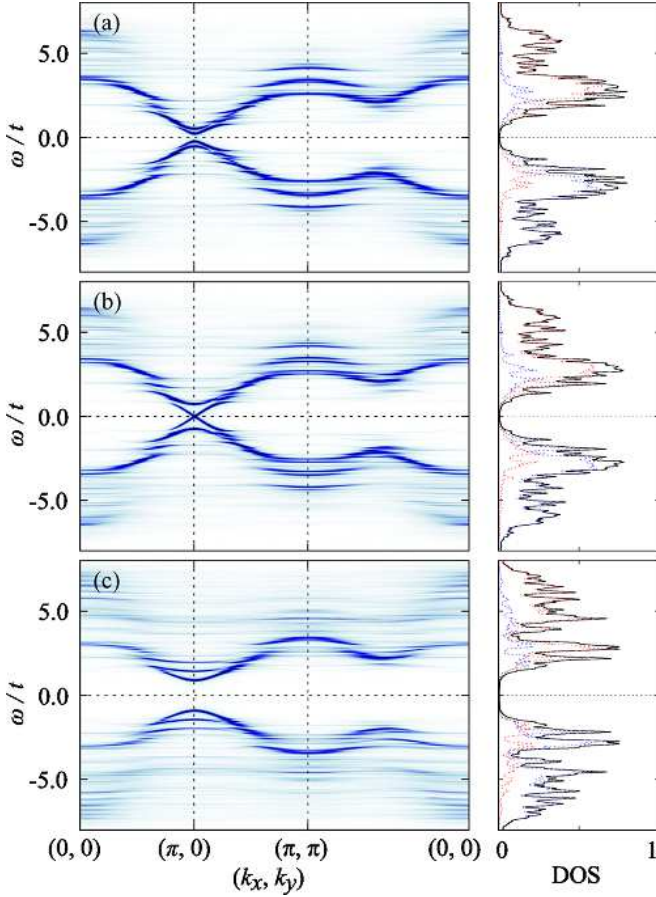


FIG. 8: (Color online) Calculated single-particle spectrum for the bulk state (left panel) and corresponding DOS with the orbital decompositions (right panel) at (a)  $U=3.54t$  (magnetic transition point), (b)  $U=3.87t$  (topological phase transition point), and (c)  $U=6.00t$  (AFMI state).

with  $\mathbf{S}_{i\alpha} = \frac{1}{2} \sum_{\tau, \tau'} c_{i\alpha\tau}^\dagger [\hat{\sigma}]^{\tau, \tau'} c_{i\alpha\tau'}$  and orbital indices  $\alpha$  and  $\beta$ . This Hamiltonian has the in-plane ferromagnetic interaction  $J_{ij; \alpha\beta}^{xy}$  coming from the spin-dependent anisotropic hopping term due to the spin-orbit coupling, and therefore, the spin space in this model does not have a full  $SU(2)$  symmetry but rather has an Ising-like axial anisotropy. In Fig. 5, we show the spin configuration which is expected to occur in this Hamiltonian. This magnetic order satisfies the spin-quantized condition, and therefore, SChN is useful for determining the topological phase transition in our BHZ model under the magnetic order. No other magnetic orders, such as the in-plane orders, than that shown in Fig. 5, have been detected, which is in contrast to the Kane-Mele model where the in-plane magnetic order occurs at the large  $U$  limit. Note that the  $\mathbb{Z}_2$  invariant is not meaningful due to the time-reversal symmetry breaking and cannot be used for determining the topological phase transition.

Let us then assume the AF order shown in Fig. 5 and use the Weiss field of the form

$$\mathcal{H}_M = h \sum_{i\alpha\tau\tau'} e^{i\mathbf{Q}\cdot\mathbf{r}_i} c_{i\alpha\tau}^\dagger [\hat{\sigma}_z]^{\tau\tau'} c_{i\alpha\tau'} \quad (9)$$

with  $\mathbf{Q} = (\pi, \pi)$  as the variational parameter in our VCA calculations. Figure 6 shows the calculated result for the grand potential as the function of the Weiss field  $h$  at several values of  $U$ . We find that there is a stationary point at  $h \neq 0$  for  $U > 3.54t$  and thus the AF state appears for  $U > 3.54t$ . We also calculate the local magnetic moment defined by

$$m_z = \frac{1}{2N} \sum_{i\alpha\tau\tau'} e^{i\mathbf{Q}\cdot\mathbf{r}_i} \langle c_{i\alpha\tau}^\dagger [\sigma^z]^{\tau\tau'} c_{i\alpha\tau'} \rangle \quad (10)$$

where  $\langle \dots \rangle$  represents the ground-state expectation value,  $N$  is the number of the sites in the supercluster, and  $\mathbf{Q} = (\pi, \pi)$ .

The calculated result for  $m_z$  is shown in Fig. 7, together with the result for SChN. We find that the magnetic transition occurs at  $U = 3.54t$ , which is of the second order (contrary to the previous DMFT study<sup>29</sup>), and that the SChN has the discontinuous change from 1 to 0 with the divergence at  $U = 3.87t$ . We thus detect the region, i.e.,  $3.54t < U < 3.87t$ , where the topologically nontrivial state coexists with the AF order, which is nothing but the AFTI state.

Figure 8 shows the results for the single-particle spectra for the bulk state with the axial AF order at several values of  $U/t$  ( $= 3.54, 3.87, 6.00$ ). We find that the behaviors similar to the nonmagnetic case (see Fig. 3) are observed also in the magnetically ordered case. We in particular confirm that the closing of the bulk gap is observed at  $U = 3.87t$  (see Fig. 8(b)), i.e., at the topological phase transition point between the two topologically distinct phases, AFTI and AFMI. In the Kane-Mele model, it is known that the bulk gap does not close at the transition point between TBI and AFMI and that there is no coexistence region between the topological order and



in-plane AF order. Our results therefore indicate the importance of the the spin quantized condition, in relation to the symmetry in spin space, the coexistence region, and the bulk band gap.

#### IV. SUMMARY

We have studied the effects of electron correlations on the topological phase transitions, focusing in particular on the presence of the antiferromagnetic topological insulator state. We have used the Bernevig-Hughes-Zhang (BHZ) model with the on-site Hubbard interaction and have applied the variational cluster approach (VCA) whereby the short-range spatial correlations are taken into account exactly. We have calculated the spin Chern number (SchN) and local magnetic moment as well as the single-particle spectra for the bulk and edge states.

In the nonmagnetic case, we found that the topological phase transition between the topological band insulator (TBI) and nonmagnetic insulator (NMI) occurs with the simultaneous vanishing of the bulk band gap and gapless edge state. This result may be a general conclusion equally valid for other topological phase transitions be-

tween TBI and NMI. We have also studied the magnetic instability of this model and have clarified the relation between the topological and antiferromagnetic (AF) orders. We have calculated the spin Chern number and the local magnetic moment of the AF ordered state and confirmed that the magnetic transition, which was found to be of the second order, and topological phase transition do not occur simultaneously, but rather the topological order coexists with the AF order in the spin-quantized condition. From the single-particle gap for the bulk state, we have demonstrated that the topological phase transition between the AF topological insulator state and AF Mott insulator state occurs when the bulk gap closes.

#### Acknowledgments

Enlightening discussions with S. Ejima, H. Fehske, Y. Fuji, and K. Seki are gratefully acknowledged. This work was supported in part by Kakenhi Grant No. 22540363 of Japan. A part of computations was carried out at the Research Center for Computational Science, Okazaki Research Facilities, Japan.

- 
- <sup>1</sup> X. G. Wen, Phys. Rev. B **40**, 7387 (1989).
  - <sup>2</sup> Y. Hatsugai, J. Phys. Soc. Jpn. **73**, 2604 (2004); **74**, 1374 (2005).
  - <sup>3</sup> D. J. Thouless, M. Kohmoto, M. P. Nightingale, and M. den Nijs, Phys. Rev. Lett. **49**, 405 (1982).
  - <sup>4</sup> M. Kohmoto, Ann. Phys. (New York) **160**, 355 (1985).
  - <sup>5</sup> M. Z. Hasan and C. L. Kane, Rev. Mod. Phys. **82**, 3045 (2010).
  - <sup>6</sup> X. L. Qi and S. C. Zhang, Rev. Mod. Phys. **83**, 1057 (2011).
  - <sup>7</sup> B. A. Bernevig and S. C. Zhang, Phys. Rev. Lett. **96**, 106802 (2006).
  - <sup>8</sup> C. L. Kane and E. J. Mele, Phys. Rev. Lett. **95**, 146802 (2005).
  - <sup>9</sup> C. L. Kane and E. J. Mele, Phys. Rev. Lett. **95**, 226801 (2005).
  - <sup>10</sup> B. A. Bernevig, T. L. Hughes, S. C. Zhang, Science **314**, 1757 (2006).
  - <sup>11</sup> S. Murakami, Phys. Rev. Lett. **97**, 236805 (2006).
  - <sup>12</sup> L. Fu and C. L. Kane, Phys. Rev. B **76**, 045302 (2007).
  - <sup>13</sup> M. König, S. Wiedmann, C. Brüne, A. Roth, H. Buhmann, L. W. Molenkamp, X. L. Qi, and S. C. Zhang, Science **318**, 766 (2006).
  - <sup>14</sup> D. Hsieh, D. Qian, L. Wray, Y. Xia, Y. S. Hor, R. J. Cava, and M. Z. Hasan, Nature **452**, 970 (2008).
  - <sup>15</sup> Y. Xia, D. Qian, D. Hsieh, L. Wray, A. Pal, H. Lin, A. Bansil, D. Grauer, Y. S. Hor, R. J. Cava, and M. Z. Hasan, Nat. Phys. **5**, 398 (2009).
  - <sup>16</sup> Y. L. Chen, J. G. Analytis, J.-H. Chu, Z. K. Liu, S.-K. Mo, X. L. Qi, H. J. Zhang, D. H. Lu, X. Dai, Z. Fang, S. C. Zhang, I. R. Fisher, Z. Hussain, and Z.-H. Shen, Science **325**, 178 (2009).
  - <sup>17</sup> A. P. Schnyder, S. Ryu, A. Furusaki, and A. W. W. Ludwig, Phys. Rev. B **78**, 195125 (2008).
  - <sup>18</sup> S. Ryu, A. P. Schnyder, A. Furusaki, and A. W. W. Ludwig, New. J. Phys. **12**, 065010 (2010).
  - <sup>19</sup> A. Kitaev, AIP Conf. Proc. **1134**, 22 (2009).
  - <sup>20</sup> L. Fu, Phys. Rev. Lett. **106**, 106802 (2011).
  - <sup>21</sup> R. S. K. Mong, A. M. Essin, and J. E. Moore, Phys. Rev. B **81**, 245209 (2010).
  - <sup>22</sup> H. Guo, S. Feng, and S.-Q. Shen, Phys. Rev. B **83**, 045114 (2011).
  - <sup>23</sup> A. Shitade, H. Katsura, J. Kunes, X.-L. Qi, S. C. Zhang, and N. Nagaosa, Phys. Rev. Lett. **102**, 256403 (2009).
  - <sup>24</sup> D. Pesin and L. Balents, Nat. Phys. **6**, 376 (2010).
  - <sup>25</sup> V. Gurarie, Phys. Rev. B **83**, 085426 (2011).
  - <sup>26</sup> Y. Yamaji and M. Imada, Phys. Rev. B **83**, 205122 (2011).
  - <sup>27</sup> M. Hohenadler, T. C. Lang, and F. F. Assaad, Phys. Rev. Lett. **106**, 100403 (2011).
  - <sup>28</sup> T. Yoshida, S. Fujimoto, and N. Kawakami, Phys. Rev. B **85**, 125113 (2012).
  - <sup>29</sup> T. Yoshida, R. Peters, S. Fujimoto, and N. Kawakami, Phys. Rev. B **87**, 085134 (2013).
  - <sup>30</sup> T. Yoshida, R. Peters, S. Fujimoto, and N. Kawakami, e-print arXiv:1301.5688v1.
  - <sup>31</sup> Y. Tada, R. Peters, M. Oshikawa, A. Koga, N. Kawakami, and S. Fujimoto, Phys. Rev. B **85**, 165138 (2012).
  - <sup>32</sup> S. L. Yu, X. C. Xie, and J. X. Li, Phys. Rev. Lett. **107**, 010401 (2011).
  - <sup>33</sup> W. Wu, S. Rachel, W.-H. Liu, and K. L. Hur, e-print arXiv:1106.0943v2.
  - <sup>34</sup> M. Hohenadler and F. F. Assaad, e-print arXiv:1211.1774v3.
  - <sup>35</sup> M. Potthoff, M. Aichhorn, and C. Dahnken, Phys. Rev. Lett. **91**, 206402 (2003).
  - <sup>36</sup> M. Potthoff, Eur. Phys. J. B **32**, 429 (2003); **36**, 335 (2003).

- <sup>37</sup> D. Sénéchal, D. Perez, and M. Pioro-Ladriere, Phys. Rev. Lett. **84**, 522 (2000).
- <sup>38</sup> M. Potthoff, in *Strongly Correlated Systems: Theoretical Methods*, edited by A. Avella and F. Mancini, Springer Series in Solid-State Sciences, Vol. 171 (Springer, Berlin, 2012), pp. 303-339.
- <sup>39</sup> D. Sénéchal, e-print arXiv:0806.2690v2.
- <sup>40</sup> G. E. Volovik, *The Universe in a Helium Droplet* (Oxford University Press, Oxford, 2003).
- <sup>41</sup> T. Fukui and Y. Hatsugai, Phys. Rev. B **75**, 121403 (2007).
- <sup>42</sup> K. Ishikawa and T. Matsuyama, Nucl. Phys. B **280**, 523 (1987).
- <sup>43</sup> F. D. M. Haldane, Phys. Rev. Lett. **93**, 206602 (2004).